Mechanical Force and Cytoplasmic Ca^{2+} Activate Yeast TRPY1 in Parallel

Zhenwei Su · Xinliang Zhou · Stephen H. Loukin · Yoshiro Saimi · Ching Kung

Abstract The ability to sense mechanical and osmotic stimuli is vital to all organisms from mammals to bacteria. Members of the transient receptor potential (TRP) ion-channel family have attracted intense attention for their involvement in mechanosensation. The yeast homologue TRPY1 can clearly be activated by hypertonic shock in vivo and by stretch force under patch clamp. Like its animal counterparts, TRPY1 is polymodal, being gated by membrane stretch force and by cytoplasmic Ca^{2+}. Here, we investigated how these two gating principles interact. We found that stretch force can induce some channel activation without cytoplasmic Ca^{2+}. Tens of micromolar Ca^{2+} greatly enhance the observed force-induced activities, with open probabilities following well the Boltzmann distribution, in which the two gating energies are summed as exponents. To map this formalism to structures, we found Ca^{2+}-binding proteins such as calmodulin or calcineurin to be unnecessary. However, removing a dense cluster of negative charges in the C-terminal cytoplasmic domain of TRPY1 greatly diminishes the Ca^{2+} activation as well as its influence on force activation. We also found a strategic point upstream of this charge cluster, at which insertion of amino acids weakens Ca^{2+} activation considerably but leaves the mechanosensitivity nearly intact. These results led to a structure–function model in which Ca^{2+} binding to the cytoplasmic domain and stretching of the membrane-embedded domain both generate gating force, reaching the gate in parallel.

Introduction

Mechanical senses are common to all creatures, from hearing, touch and balance in animals to gravitropism in plants and osmotic regulation in fungi and bacteria (Kung 2005; Martinac et al. 2008). These processes involve converting different forms of mechanical stimuli into electrical signals by force-sensitive molecular transducers. Such transducers in prokaryotes are exemplified by the extensively characterized bacterial mechanosensitive ion channels of large conductance (MscL) and small conductance (MscS), which protect bacteria from osmotic downshock (Martinac et al. 2008). However, in eukaryotes, the molecular identities of such force-transducing channels are often elusive. Members of the transient receptor potential (TRP) ion channel family are apparently involved in mechanosensation. For example, human TRPP1 and TRPP2 are proposed to sense fluid flow in kidney, rat TRPV4 responds to hypotonic swelling, fly TRPVs *Nanchung* and *Inactive* function in hearing and the worm TRPV (Osm-9) is required for nose touch and hypertonic stress (Christensen and Corey 2007). Yet, whether these animal channels are the first-line force sensors or downstream amplifiers or serve other roles in mechanosensation remains unclear. In contrast, the yeast TRP channel, TRPY1, expressed in the vacuolar membrane, is clearly a mechanically sensitive molecule. It is activated not only by

Z. Su · X. Zhou · S. H. Loukin · Y. Saimi · C. Kung (✉)
Laboratory of Molecular Biology, University of Wisconsin–Madison, 305 R. M. Bock Laboratories, 1525 Linden Drive, Madison, WI 53706, USA
e-mail: ckung@wisc.edu

C. Kung
Department of Genetics, University of Wisconsin–Madison, Madison, WI 53706, USA

osmotic up-shock in vivo (Denis and Cyert 2002) but also by membrane stretch under patch clamp (Zhou et al. 2003), making it a useful model for eukaryotic primary mechanotransducers. In addition, TRPY1 requires no heterologous expression, exhibits a large 300-pS signal over noise (Palmer et al. 2001; Zhou et al. 2003) and can easily be manipulated by genetics (Su et al. 2007; Zhou et al. 2007).

Most TRP channels are polymodal. They respond to a variety of stimuli including voltage, temperature, pH and chemicals, besides mechanical force (Venkatachalam and Montell 2007). One of the most physiologically important second messengers, intracellular free Ca^{2+}, has been reported to modulate many TRP channels. For instance, TRPM2 requires Ca^{2+} for activation (McHugh et al. 2003). TRPM4 and TRPM5 both exhibit Ca^{2+} activation and subsequent inactivation, with calmodulin being required for TRPM4 but not TRPM5 (Hofmann et al. 2003; Launay et al. 2002; Nilius et al. 2005). TRPA1 is proposed to be directly activated by Ca^{2+} through an N-terminal EF-hand structure (Doerner et al. 2007; Zurborg et al. 2007), although a recent study has now challenged EF-hand's being the Ca^{2+} sensor (Wang et al. 2008). TRPY1 has been known to be activated by cytoplasmic Ca^{2+} since the registry of its channel activity (Bertl and Slayman 1990; Wada et al. 1987), long before its molecular identification (Palmer et al. 2001). Since the discovery of its mechanosensitivity under patch clamp, the action of Ca^{2+} is now thought to be an integral component in a Ca^{2+}-induced Ca^{2+} release (CICR) positive feedback that amplifies its response to mechanical force (Zhou et al. 2003).

A central issue in the study of polymodal ion channels is to clarify how different stimuli reach the same channel gate. Understanding how different stimuli act and interact in gating can lead to clear insights. For example, distinguishing the action of menthol from coolness on TRPM8 (Bandell et al. 2006) and that of warmth from camphor on TRPV3 (Grandl et al. 2008) have shed light on chemo- and thermosensitivity. To use TRPY1 to understand the mechanosensitivity in eukaryotes, we need to sort out the relation between stretch force and Ca^{2+} in gating this channel, as this study sets out to do.

Materials and Methods

Yeast Strains and Cultures

Except for the calmodulin mutant and its parent, the wild-type parental strains were BY4742 (*MATα his3Δ leu2Δ lys2Δ ura3Δ*) and *yvc1Δ* mutant (a chromosomal knockout strain, YOR088 W; *yvc1::km*). For the calmodulin experiments, calmodulin wild-type strain *CMD1*+ and calmodulin mutant strain *cmd1-6* were in the CYR1 background and were kindly provided by Dr. T. N. Davis (Geiser et al. 1991). For electrophysiology, standard yeast medium with yeast extract, peptone and dextrose (YPD) was used. For luminometric experiments, complete minimal medium with dextrose (CMD) or a modified version with ammonium chloride replacing ammonium sulfate (DCD) was used (Denis and Cyert 2002; Su et al. 2007; Zhou et al. 2007).

Mutagenesis

All site-directed mutagenesis experiments were performed using the standard overlap extension PCR method (Ho et al. 1989). Different PCR fragments carrying the corresponding mutations were cloned into HindIII/XhoI sites of *YVC1* (the gene that encodes TRPY1 protein) in a prYVC plasmid carrying a *GPD* promoter and a *URA3* marker. All mutants were verified by sequencing. Sequenced plasmids were linearized by EagI/MluI before transforming into *yvc1Δ* for gene integration. Transformed yeast mutant strains with correct markers were sequenced again from the genome to verify the *yvc1*-mutant integrants. All experiments were performed on the wild type or these integrants.

Luminometry

Luminometric measurements were conducted as previously described (Batiza et al. 1996; Denis and Cyert 2002). Briefly, yeast cells were transformed with pEVP11/AEQ plasmid bearing the apoaequorin gene and a *LEU2* marker. Transformants were selected on CMD-LEU plates. Colonies were picked and precultured in DCD-LEU medium at 30°C for 24 h and then subcultured in fresh medium supplemented with 2 μM coelenterazine for 24 h in the dark, before the up-shock-induced luminescence was measured. Cells (20 μl) were shocked with 200 μl hypertonic solutions (0.75–2.5 M NaCl, 50 mM MES [pH 7], 25 mM EGTA), and the luminescence was recorded with a Berthold LB 9507 luminometer (Berthold Detection Systems, Oak Ridge, TN).

Solutions

For patch-clamp recordings, the pipette solution contained the following (in mM): 150 KCl, 5 $MgCl_2$, 100 sorbitol, 10 HEPES-KOH, pH 7.2. The bath solution contained 150 KCl, 5 $MgCl_2$, 100 sorbitol, 10 HEPES-KOH (pH 7.2) and different Ca^{2+} concentrations adjusted by $CaCl_2$ and EGTA. For $[Ca^{2+}]$ above 10^{-5} M, $CaCl_2$ was directly added to EGTA-free bath solution. For $[Ca^{2+}]$ below 10^{-5} M, appropriate amounts of $CaCl_2$ recommended by MaxChelator (www.stanford.edu/~cpatton/maxc.html) were added to the bath solution containing 2 mM EGTA.

Electrophysiology

Yeast vacuoles were generated as previously described (Su et al. 2007; Zhou et al. 2007). All patch-clamp recordings were performed with Clampex 10.0 (Axon Instruments, Union City, CA). Data were sampled at 5 kHz and filtered at 1 kHz. Glass pipettes (100 µl; Drummond Scientific, Broomall, PA) were pulled with a P-97 Micropipette Puller (Sutter Instrument, Novato, CA) to 3–5 MΩ tip resistance. With negative pressure in the pipette, 2–3 GΩ seals were formed before being broken by transient voltage pulses to reach the whole-vacuole mode. Whole-vacuole mode patches were subsequently excised into the cytoplasmic side–out mode. Data were acquired at −30 mV voltage, with the vacuolar side being positive. Bath perfusion was used to change [Ca^{2+}]. Mechanical stimulation was applied as pressure exerted with a 60-ml syringe and gauged with an Omega (Stamford, CT) PX140 pressure sensor. Experiments were performed at room temperature (21–23°C). Data were analyzed using Clampfit 10.0 (Axon Instruments) and Microsoft (Redmond, WA) Excel. Data are presented as the mean ± SD. Significant differences were tested using Student's unpaired t-test ($P < 0.05$).

Curve Fitting for P_o vs. Pressure at Different [Ca^{2+}]

We first generated the predictions from the parallel model and then assessed how well they fit the data. The gating energy for force activation is $\Delta G_{\text{Force}} = (\gamma - \gamma_0)\,\Delta A$, where γ is the membrane tension, γ_0 the tension for half maximum activation and ΔA the change in area between the closed and the open states. The gating energy for Ca^{2+} activation is $\Delta G_{\text{Ca}} = k_{\text{B}}\,T \ln{(K_{\text{m}}\,[\text{Ca}^{2+}]^n)}$, where $k_{\text{B}}T$ has its usual meaning, K_{m} is the equilibrium constant of Ca^{2+} binding and n is the number of Ca^{2+} ions bound per channel. The parallel model dictates that $P_o/(1-P_o) = \exp{[(\Delta G_{\text{Force}} + \Delta G_{\text{Ca}})/k_{\text{B}}\ T]} = \exp{\{[(\gamma - \gamma_0)\ \Delta A + k_{\text{B}}\ T\ \ln{(K_{\text{m}}[\text{Ca}^{2+}]^n)}]/k_{\text{B}}T\}}$. The tension ($\gamma$) is directly proportional to the applied pressure (P) according to the Young–Laplace equation as the geometry of the patch is constant within one patch. Thus, further transformation converted the Boltzmann equation into $P_o/(1-P_o) = \exp{(a\,P + b)}$. For each [Ca^{2+}], the rises of P_o over the range of P in Fig. 1a were fitted to this equation with a and b being the fitting parameters (Fig. 1b). In this equation, the a values are dictated by ΔA and by the geometry of the patch, both of which remain constant within the same patch. Therefore, constancy of the a values at different [Ca^{2+}] is supportive of the parallel model. On the other hand, the b values should correlate linearly with log [Ca^{2+}], if the parallel model is correct. The a values in the fits from different [Ca^{2+}] were evaluated for constancy and the b values were evaluated for linearity against log [Ca^{2+}] (Fig. 1d). The

curve fitting was carried out using SigmaPlot 10 (Systat, Richmond, CA).

Results

Activation of TPRY1 by Membrane Stretch Force and by Ca^{2+}

We assessed the relation between stretch-force activation and Ca^{2+} activation repeatedly using patch clamp in excised cytoplasmic-side–out configuration. Results from a representative experiment that covers a large range of [Ca^{2+}] and stretch force are shown in Fig. 1. In the virtual absence of Ca^{2+} (10^{-9} M, Fig. 1a, bottom trace), there is nearly no spontaneous channel activity. Strong membrane stretches (e.g., by 240 mmHg pressure), however, can activate the channels, albeit weakly, showing that the mechanosensitivity of TRPY1 does not have an absolute dependence on the presence of cytoplasmic Ca^{2+}. This mechanosensitivity is consistent with the function of TRPY1 in vivo, which must start to open upon osmotic stress from a resting steady state with very little free Ca^{2+} in the cytoplasm. Pressures higher than 240 mmHg tend to break the patch seals and cannot practically be examined in our system. Increasing [Ca^{2+}] promotes the baseline open probability (P_o) in the absence of applied pressure, with a sharp rise between 10^{-4} and 10^{-3} M Ca^{2+}, from $P_o \sim 0.1$ to $P_o \sim 0.6$ (Fig. 1a). Furthermore, the pressure-induced P_o rises steeply with the increase in [Ca^{2+}] (Fig. 1a, top three traces). Channel activation by applied pressure is plotted in Fig. 1b for different [Ca^{2+}]. A robust pressure-induced response starts to be evident at [Ca^{2+}] above 10^{-5} M (Fig. 1a, second trace, b), and when [Ca^{2+}] approaches 10^{-3} M, this response is masked by the prominent Ca^{2+}-induced basal activities (Fig. 1a, top trace, b). Comparison of P_o with or without the application of pressure (240 mmHg) at different [Ca^{2+}] shows an apparent synergistic effect (Fig. 1c). That is, the pressure-induced P_o increase at 10^{-5} M Ca^{2+} is much larger than that at 10^{-7} M Ca^{2+}, an effect that cannot be ascribed to the Ca^{2+}-induced P_o increase alone.

In simplified models, the gating force from Ca^{2+} binding and that from membrane stretch can work in series or in parallel. In a serial model, Ca^{2+} binding may be viewed as a prerequisite step for stretch-force sensing. Such a model is not supported by our data because TRPY1 remains mechanically sensitive in the virtual absence of Ca^{2+} (Fig. 1a, bottom trace). In a parallel model, two stimuli are independently sensed and transmitted to the gate. The integration of the two influences can be evaluated by the sum of the two energy exponents. As given in "Materials and Methods," this model converts the Boltzmann equation into
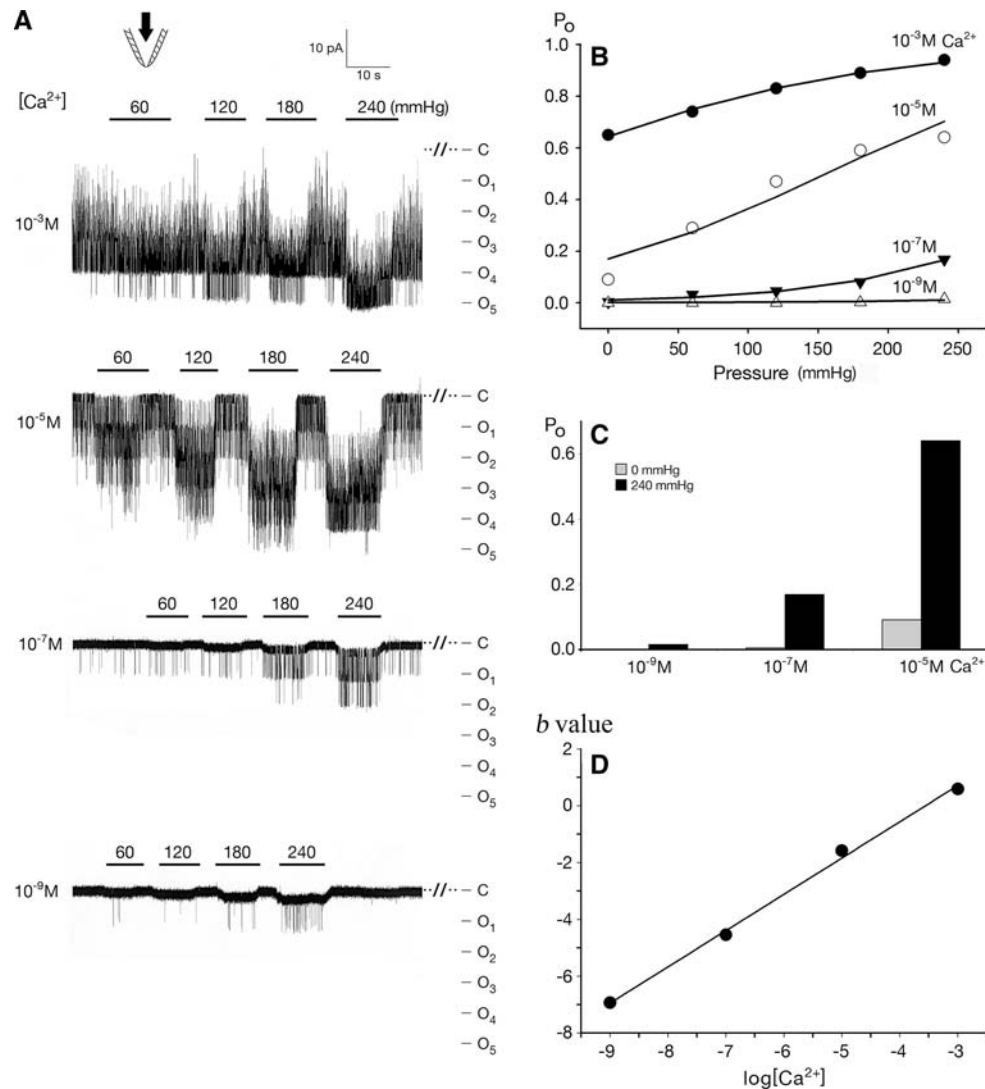
Fig. 1 Relationship between TRPY1's mechanosensitivity and Ca^{2+} sensitivity. **a** One representative recording from repeated studies displays channel activities in response to four different pressures (60, 120, 180 and 240 mmHg, *left* to *right*) at four different $[Ca^{2+}]$ (10^{-9}, 10^{-7}, 10^{-5} and 10^{-3}, *bottom* to *top*). All patch-clamp recordings were performed on isolated vacuoles in excised cytoplasmic side–out configuration at -30 mV (vacuolar side positive). In the absence of Ca^{2+} (10^{-9} M), channels are weakly activated by strong pressure (240 mmHg) (*bottom trace*). Above 10^{-7} M Ca^{2+}, force-induced responses become evident. At a high $[Ca^{2+}]$ (10^{-3} M), robust basal Ca^{2+}-induced activities mask most of the pressure responses. **b** P_o vs. pressure at different $[Ca^{2+}]$, from the data shown in **a** fitted with Boltzmann curves. **c** Comparison of P_o with or without the application of 240 mmHg pressure at different $[Ca^{2+}]$ shows a synergistic effect. Note, the pressure-induced P_o increase at 10^{-5} M Ca^{2+} is much larger than that at 10^{-7} M Ca^{2+}. **d** Plot of the b value vs. log $[Ca^{2+}]$. The b value, a curve-fitting parameter, shows a linear correlation with log $[Ca^{2+}]$ predicted by the parallel model. See "Materials and Methods"

$P_o/(1-P_o) = \exp(a\,P + b)$. This equation was used to fit the actual data points shown in Fig. 1b, with a and b being the fitting parameters. The a values from the fits were found to be 0.012, 0.010 and 0.008 for 10^{-7}, 10^{-5} and 10^{-3} M Ca^{2+}, respectively. For 10^{-9} M Ca^{2+} the a value could not be accurately given due to the extreme low activity. Thus, the a values show a reasonable constancy, being 0.01 ± 0.002 (mean $\pm$ SD), supporting the parallel model. The b values were plotted with log $[Ca^{2+}]$ in Fig. 1d, showing b vs. log $[Ca^{2+}]$ being linear, also in favor of a parallel model. In this model, the apparent synergism between force activation and Ca^{2+} activation in TRPY1 can be attributed to the sum of the two exponents of gating energies.

Common Ca^{2+}-Binding Proteins such as Calmodulin and Calcineurin are not Required for Ca^{2+} Activation of TRPY1

The synergistic effect between force sensitivity and Ca^{2+} sensitivity encouraged us to further investigate the Ca^{2+}

activation of TRPY1 in structural terms. Since many known Ca^{2+}-activated ion channels are regulated through Ca^{2+}-binding protein partners, we asked whether this is the case with TRPY1. Osmotic up-shocks activate TRPY1 in vivo to release Ca^{2+} from the vacuole into the cytoplasm, which can be measured by transgenic aequorin (Batiza et al. 1996; Denis and Cyert 2002). We have surveyed a collection of 4,810 yeast single-gene deletion strains for their TRPY1-dependent osmotic up-shock responses in search for possible interacting elements that regulate TRPY1 (Loukin et al. 2008). Deletions of most Ca^{2+}-related proteins, such as the well-known CaM kinases, do not significantly affect TRPY1's hypertonic response. The calcineurin deletant *cnb1*, which lacks the Ca^{2+}-binding calcineurin B subunit, however, has a higher vacuolar $[Ca^{2+}]$ and consequently an exaggerated Ca^{2+} response but no clear alteration of TRPY1's channel behaviors under patch clamp (Loukin et al. 2008). Therefore, it is unlikely that calcineurin regulates TRPY1's Ca^{2+} gating process. One caveat of the screen is that vital genes are not included in the deletion collection and the calmodulin gene is among them.

Calmodulin is a prominent candidate since it is known to be the Ca^{2+}-binding subunit in many channels including several TRPs (Nilius et al. 2004, 2005; Saimi and Kung 2002). The *Saccharomyces cerevisiae* genome has a single calmodulin gene, *CMD1*. *CMD1* is vital. However, the mutant *cmd1-6*, with multiple mutations engineered to remove all of CMD1's ability to bind Ca^{2+}, grows normally (Geiser et al. 1991). We therefore used *cmd1-6* to test whether Ca^{2+}-calmodulin is needed to activate TRPY1. The Ca^{2+} responses upon 1.5 M NaCl osmotic up-shock from *cmd1-6* and its parent $CMD1^+$ are not significantly different (Fig. 2a). The normalized peak responses to up-shocks, ranging 0.75–2 M NaCl, are also not significantly different between the two (Fig. 2b). We also directly examined the activities of TRPY1 channels in *cmd1-6* and $CMD1^+$ vacuoles with patch clamp. Ensemble currents at different $[Ca^{2+}]$ appear similar between the two (Fig. 2c, d). Mechanosensitivity of the channels, as assessed in excised cytoplasmic side–out patches under 120 mmHg pressure, also appears to be unaffected by the *cmd1-6* mutation (Fig. 2c, d). Although sizable variations may obscure
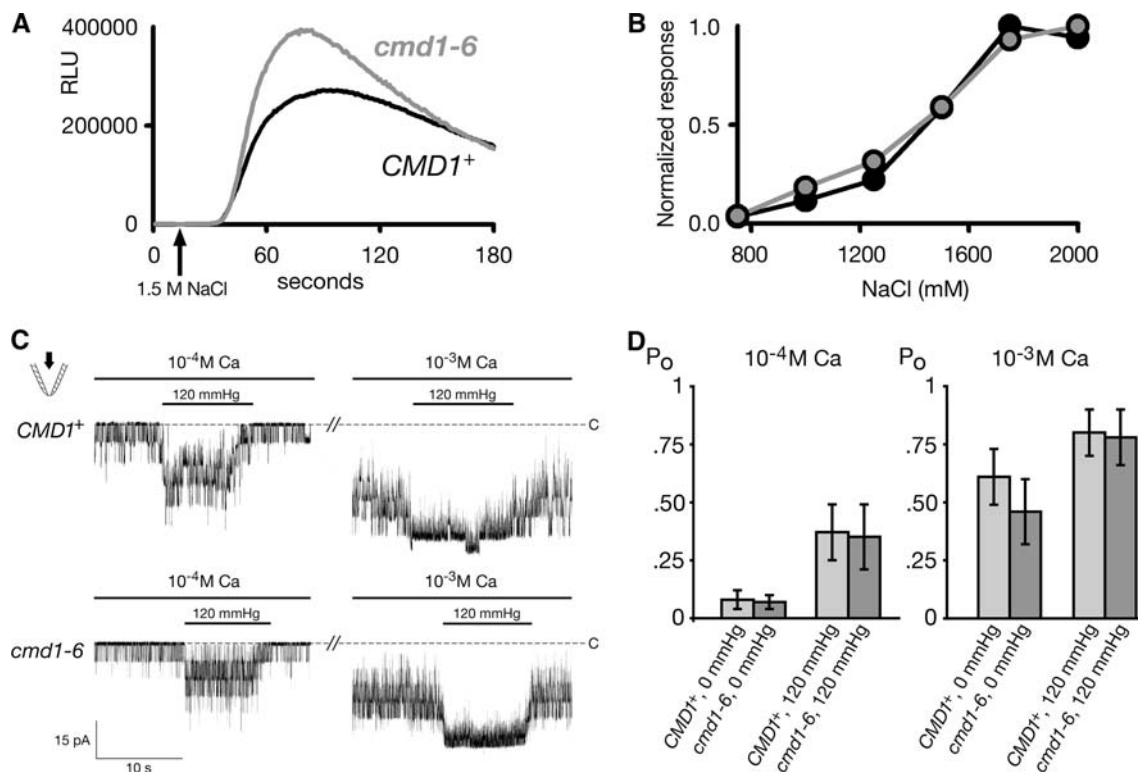

Fig. 2 Ca^{2+}-calmodulin is not required for the Ca^{2+} activation of TRPY1. **a** Osmotic up-shock-induced Ca^{2+} releases of calmodulin mutant *cmd1-6* (*gray*) and its parent $CMD1^+$ (*black*) are not significantly different. *Arrow* indicates the addition of 1.5 M NaCl. Luminescence was gauged as relative light units (RLUs) with transgenic aequorin. **b** Normalized peak responses to the shocks of different concentrations of NaCl (0.75–2 M) of *cmd1-6* (*gray*) and $CMD1^+$ (*black*) appear similar. **c** Patch-clamp recordings of $CMD1^+$ (*top traces*) and *cmd1-6* (*bottom traces*) at 10^{-4} M Ca^{2+} (*left traces*) and 10^{-3} M Ca^{2+} (*right traces*) do not differ prominently. Pressure of 120 mmHg was applied as indicated. **d** Averaged responses show no statistically evident difference between the calmodulin mutant ($n = 10$) and its parent ($n = 6$). Mean ± SD

individual differences (note SD Fig. 2d), it seems clear that Ca^{2+}-calmodulin is not a direct partner in TRPY1's Ca^{2+} activation. Thus, our screen and mutant analyses suggest that Ca^{2+} probably directly activates TRPY1.

A C-Terminal Negative Charge Cluster is Needed for TRPY1's Ca^{2+} Activation

We next tried to find structural elements within the TRPY1 protein that may be required for Ca^{2+} activation. Analyses showed no well-recognized Ca^{2+}-binding motifs such as EF-hand or RCK domains in TRPY1. A cluster of acidic amino acids, however, can be found in the presumed C-terminal cytoplasmic domain of the predicted TRPY1 subunit structure (Fig. 3a, residues 555–582). The strongest negative density is four consecutive aspartates (^{573}DDDD^{576}), and we engineered an 11-residue deletion, Δ570–580, removing the ^{570}GYLDDDDGLFS^{580} peptide to examine the possible functional significance of these negative charges. Luminometric measurements showed

that Δ570–580 has no evident response above TRPY1 knockout control (Fig. 3b). We further used patch clamp to directly compare the channel activities of Δ570–580 with those of the wild type. In multiple studies using excised cytoplasmic-side–out patches, the mutant activities are found to be drastically diminished. As shown in Fig. 3c (left), when bathed in 10^{-4} M Ca^{2+}, the steady-state activities as well as the pressure-induced activities of the wild type are evident but the activities of Δ570–580, though present, are almost completely lost. In 10^{-3} M Ca^{2+} (Fig. 3c, right), the wild-type channels are highly active and approach maximum when pressure is applied. The Δ570–580 again showes significantly reduced basal activity, although activation by stretch force is evident. It should be noted that, although weak, residual Ca^{2+} activation clearly remains in Δ570–580. The activities of Δ570–580 at 10^{-4} M Ca^{2+} (Fig. 3c, lower left) are similar to those of wild type at 10^{-9} M Ca^{2+} (Fig. 1a, bottom trace), whereas the activities of Δ570–580 at 10^{-3} M Ca^{2+} resembles those of the wild type at 10^{-7} M Ca^{2+}
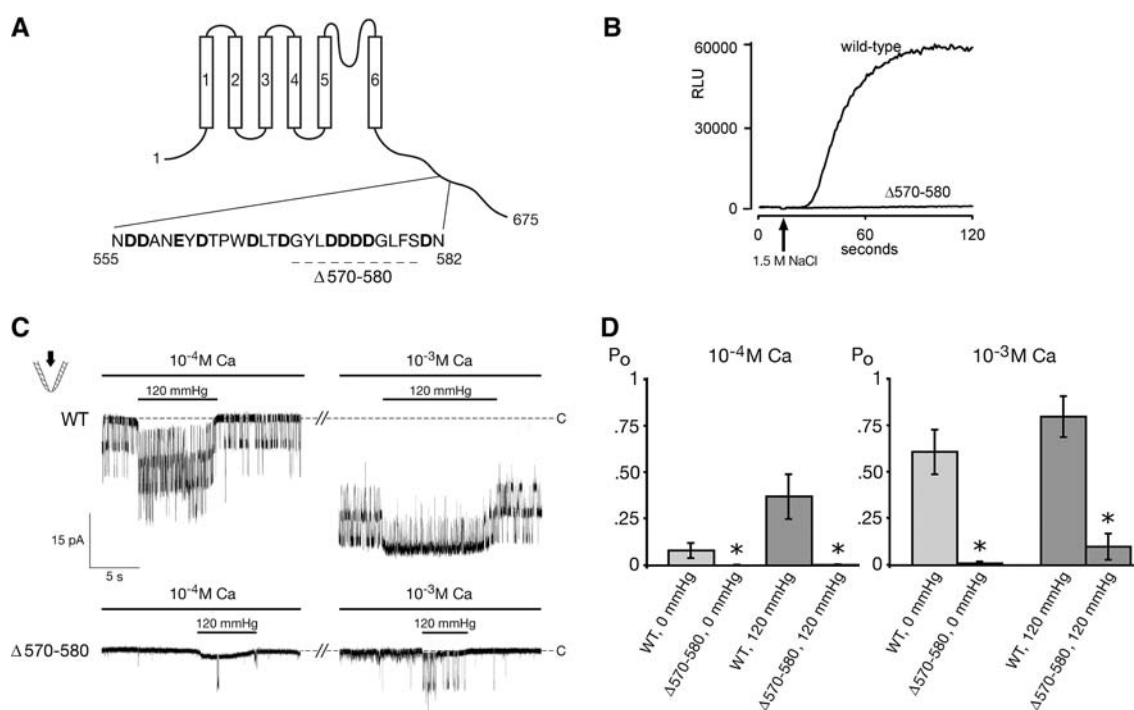

Fig. 3 A dense cluster of negative charges in the C-terminal cytoplasmic domain is required for Ca^{2+} activation. **a** Schematic representation of a single channel subunit with six transmembrane helices, N- and C-terminal cytoplasmic domains. A cluster of negative charges in the C-terminal cytoplasmic domain (residues 555–582) is shown, with negative charges in bold. A deletion of 11 amino acids (Δ570–580) within this cluster encompassing the strongest negative charge density ^{573}DDDD^{576} is indicated by a *dashed line*. **b** In vivo osmotic up-shock-induced luminometric responses of wild type and Δ570–580. NaCl, 1.5 M, elicits a robust signal from wild type, whereas in Δ570–580 there is no clear response

above *TRPY1* knockout control. **c** Patch-clamp recordings of wild type (WT, *top traces*) and Δ570–580 (*bottom traces*) at 10^{-4} M Ca^{2+} (*left traces*) and 10^{-3} M Ca^{2+} (*right traces*). In contrast to the wild type's robust response to both applied pressure and Ca^{2+} at the tested conditions, the Δ570–580 mutant shows much reduced Ca^{2+}-induced activities even at high [Ca^{2+}] and its observed pressure-induced activities are also weakened. **d** Comparison of the P_o of the wild-type and the Δ570–580 mutant at 10^{-4} M Ca^{2+} (*left*) and 10^{-3} M Ca^{2+} (*right*) with or without 120 mmHg pressure. Mean ± SD ($n = 10$ for wild type and $n = 5$ for Δ570–580) (*$P < 0.001$)

(Fig. 1a, third trace). This retained Ca^{2+} activation in Δ570–580 accounts for its increased force responses at a higher [Ca^{2+}] (10^{-3} M). The statistical loss of P_o in Δ570–580 is shown in Fig. 3d for comparison. This loss may be underestimated since the true number of conducting units in the patch cannot be estimated for the mutant due to its low activities. It is clear that Δ570–580 not only largely diminishes Ca^{2+} activation but also weakens the synergistic effect on force activation. Thus, the lack of in vivo responses in Δ570–580 (Fig. 3b) could result from not enough activities to trigger and maintain a CICR feedback pathway in the presence of Ca^{2+}

sequestering machineries in yeast cells. These results show that Ca^{2+} activation likely initiates from the direct binding of Ca^{2+} to TRPY1 itself and the cluster of negative charges here may be necessary for that binding.

Inserted Residues Result in Selective Attenuation of Ca^{2+} Activation

A sequence analysis of TRPY1 shows that there are two patches of high hydrophobicity (HP1 and HP2 in Fig. 4a) between the negative-charge cluster and the end of S6. HP1
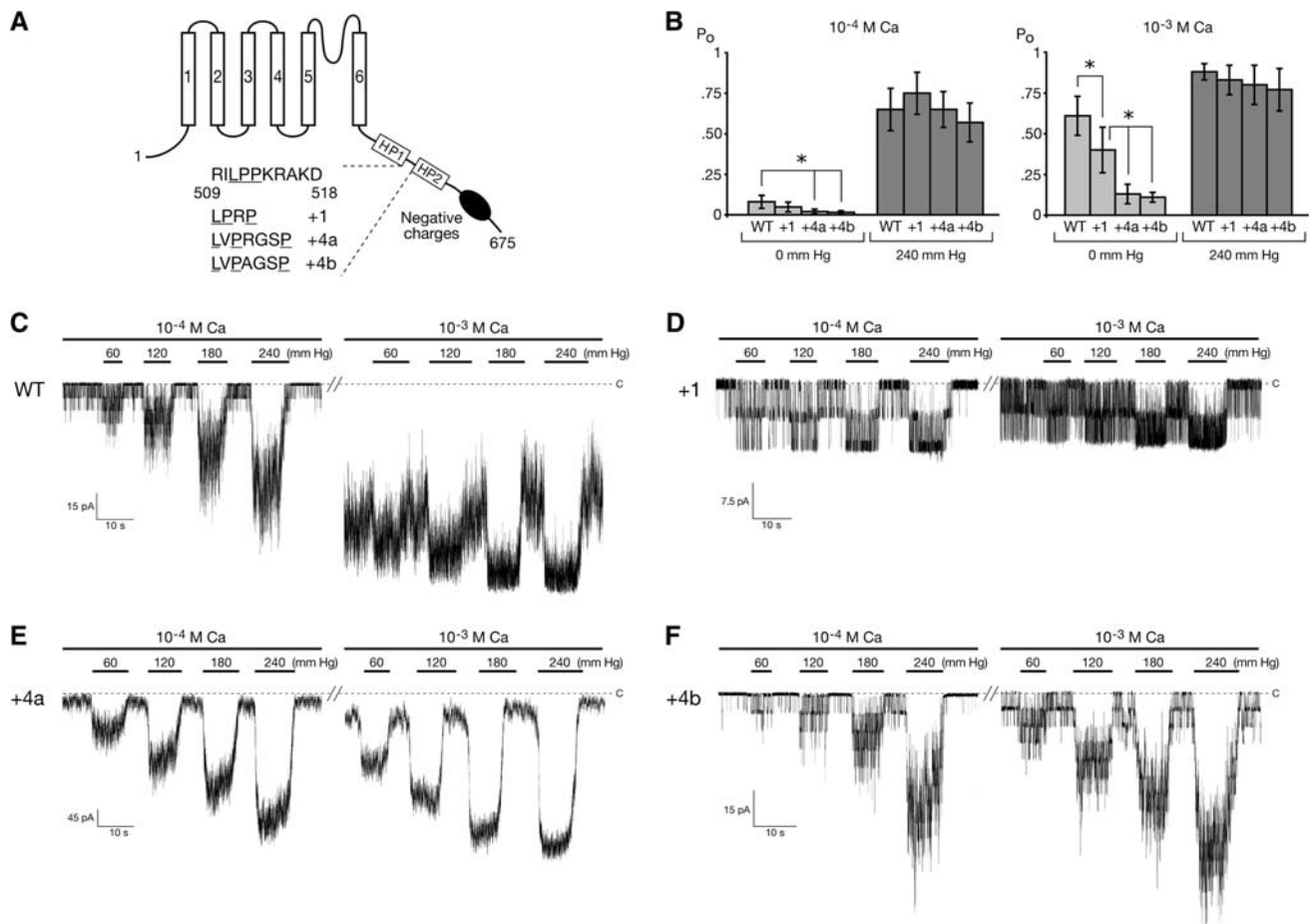

Fig. 4 Inserted residues result in selective decrement of Ca^{2+} activation. **a** Schematic representation shows structural motifs between S6 and the negative charge cluster. Two hydrophobic patches (HP1 and HP2) are predicted by hydrophilicity plot. They are connected through residues 509–518. Three different insertion mutations were constructed at this site: +1 mutant adds R after P^{512}, +4a mutant adds V after L^{511} as well as RGS after P^{512}, +4b mutant adds V after L^{511} and AGS after P^{512}. **b** Comparison of the P_o of the wild-type (WT) and the three insertion mutants at 10^{-4} M Ca^{2+} (*left*) and 10^{-3} M Ca^{2+} (*right*) with or without 240 mmHg pressure. The insertion mutants display selective reduction of Ca^{2+} activation and nearly normal pressure activation. Mean ± SD (WT, $n = 10$; +1,

$n = 5$; +4a, $n = 10$; +4b, $n = 4$) (*$P < 0.05$) **c–f** Patch-clamp recordings of channel activities from wild type, +1, +4a and +4b at 10^{-4} M Ca^{2+} (*left*) and 10^{-3} M Ca^{2+} (*right*). Different pressures were exerted as indicated. Wild type exhibits pronounced baseline activities at 10^{-3} M Ca^{2+} without added pressure, and this robust activation masks most pressure-induced responses. Two +4 mutants significantly reduce the basal activity at 10^{-3} M Ca^{2+} and therefore unveil the observed mechanosensitivity. The +1 mutant displays a milder decrement of Ca^{2+} activation at 10^{-3} M. (The apparent difference between **d** and **e** is due to the numbers of channels in the patches)

and HP2 are connected through [509]RILPPKRAKD[518]. We added four residues, converting [511]LPP[513] to LVPRGSP, to create a thrombin-cutting site. This construct, now called "+4a" (Fig. 4a), did not show the phenotype in the intended thrombin-cleavage experiment (data not shown) but produced an inadvertent but illuminating effect. Under patch clamp, the baseline activities (without pressure) of +4a are considerably lower than the wild type, with the difference being more evident at a higher $[Ca^{2+}]$ (10^{-3} M) (Fig. 4b, c, e, *$P < 0.05$). It should be noted that, compared with the negative-charge deletion $\Delta570–580$ (Fig. 3c, d), the loss of Ca^{2+} activation in +4a is much less severe (Fig. 4b, e). Interestingly, the mechanosensitivity of +4a is nearly intact (Fig. 4b, e). It appears that the Ca^{2+} activation retained in +4a confers sufficient synergism to enable the observed force-induced activities to be nearly normal, resembling the activities of wild type at 10^{-5} M Ca^{2+} (Fig. 1a, second trace). To test whether the selective reduction of Ca^{2+} activation is due to the specific sequence of the thrombin-cutting site, we replaced its key charged arginine with the small and uncharged alanine, changing the sequence to LVPAGSP to create the "+4b" construct (Fig. 4a). Under patch clamp, +4b behaves similarly to +4a (Fig. 4b, f). Both the +4a and +4b mutants have evidently lessened Ca^{2+}-induced activities, but their activations by pressure are nearly normal. Note that, to assess the P_o of +4a and +4b, we used 10^{-3} M Ca^{2+} together with 240 mmHg pressure to estimate the total number of conducting units. The channel activities in this condition may not be saturated, especially for +4b mutant (Fig. 4e, f), and therefore their normalized P_o values may be slightly underestimated. However, this underestimation does not affect our conclusion since it is very evident that at 10^{-3} M Ca^{2+} the basal activities are much lower than the response under 240 mmHg pressure in +4a and +4b (Fig. 4e, f), compared with the robust baseline activities of wild type in the same condition and its masking effect on further force responses (Fig. 1a, top trace, 4c). Finally, to test whether the length of the linker is a determinant, we generated a construct with the insertion of only one residue, "+1", converting [511]LPP[513] to LPRP (Fig. 4a). Interestingly, the +1 mutant shows clearly milder decrement of basal activities than the two +4 mutants and has little influence on mechanosensitivity (Fig. 4b, d), as is the case with the +4 mutants. This selective loss of Ca^{2+} activation in the insertion mutants is consistent with the idea that the point of insertion is in the transmission path of the Ca^{2+}-gating force. Although the true mechanism is yet to be clarified, amino acid insertions may slacken the transmission path. Since mechanical activation is not greatly affected by the inserted residues, this transmission appears separable from that of the membrane stretch force that also reaches the gate, further supporting a parallel model.

Discussion

In this study, we investigated the relationship between stretch-force activation and Ca^{2+} activation in the polymodal ion channel TRPY1. Polymodal gating is a common feature in many ion channels. For instance, TRP channels are regulated by voltage, temperature, force, pH and chemicals (Pedersen et al. 2005; Ramsey et al. 2006; Venkatachalam and Montell 2007); tandem pore-domain potassium channels are modulated by force, polyunsaturated fatty acids and pH (Honore 2007); MscS is gated by force, voltage and protons (Hurst et al. 2008); large-conductance Ca^{2+}-activated K^+ (BK) channels are activated by voltage and Ca^{2+} (Cox et al. 1997; Horrigan and Aldrich 2002; Latorre and Brauchi 2006; Magleby 2003). A fundamental question in polymodal channels is how different sorts of physical and chemical stimuli act and interact. Extensive efforts, including mutations and chimeras, have been devoted to solve the relationships among the gating principles (Bandell et al. 2006; Grandl et al. 2008; Honore 2007; Latorre and Brauchi 2006; Magleby 2003; Voets et al. 2004).

Our results shed light on TRPY1's Ca^{2+} sensitivity, which is different from that of known Ca^{2+}-activated TRP channels. Many Ca^{2+}-activated TRP channels are reported to require calmodulin as a regulatory subunit (Nilius et al. 2004, 2005; Saimi and Kung 2002). Thus far, only one TRP channel, TRPA1, has been definitively proposed to be directly activated by Ca^{2+}, although the location of its Ca^{2+} sensor is still under debate (Doerner et al. 2007; Wang et al. 2008; Zurborg et al. 2007). By screening the yeast deletion collection and by examining the yeast calmodulin mutant (Fig. 2), we excluded common Ca^{2+}-binding proteins being involved in regulating TRPY1's Ca^{2+} sensitivity. Our work indicates that TRPY1 is probably directly activated by Ca^{2+}. Intriguingly, there are no well-known Ca^{2+}-binding motifs such as EF-hand, RCK domain or BK-like Ca^{2+} bowl in TRPY1. Thus, a novel Ca^{2+}-binding structural element may be at work. We found a dense cluster of negative charges to be necessary for Ca^{2+} activation (Fig. 3). They likely contribute to a part of Ca^{2+} binding, although the nature of the binding site awaits structural information in the future.

With regard to the mechanosensitivity in TRP channels, the yeast TRPY1 provides a model to scrutinize the relationship between force and Ca^{2+} activation. In theory, these two gating principles can work in series or in parallel. In a serial model, force could be detected by steady-state force sensors and exerts its effect by modifying the Ca^{2+} sensor conformations and thereby increasing the Ca^{2+} binding affinity, or alternatively, Ca^{2+} binding could result in subsequent formation of transient force sensors that could further perceive the addition of membrane stretch. In

such possibilities of the serial model, Ca^{2+} activation can be viewed as a prerequisite step before force activation. In contrast, a parallel model describes different stimuli being sensed and transmitted to the gate independently and different forms of energy can be summed as Boltzmann factors at the channel gate to produce a synergistic effect. Although these two types of models may oversimplify the true gating mechanism, discriminating between them can provide insights. In our study, we found evidence supporting that force and Ca^{2+} act in parallel and these two gating stimuli operate independently and synergistically on TRPY1. Ca^{2+} activates this channel without added stretch force. Strong stretch force can also induce channel activities in the virtual absence of cytoplasmic Ca^{2+}. Note, unlike Ca^{2+}, the application of stretch force is limited by the strength of patch seals. Within the range we can test, stretch-force responses in the presence of cytoplasmic Ca^{2+} fit well to an a priori Boltzmann equation by summing the two energy exponents (Fig. 1). It is of interest to evaluate the binding constant (K_m) and the number of bound Ca^{2+} (n) from existing data. However, because of membrane–glass adhesion as well as surface tension and other forces innate to the lipid bilayer, it is likely that there is mechanical energy impinging on the gate even when no added tension is applied to the patch. Because the inability to experimentally set the mechanical energy term to zero, the mechanical contribution to gating energy cannot be practically sorted out from that of Ca^{2+} binding and, therefore, the K_m and n of Ca^{2+} activation cannot be accurately extracted from existing data. The energetic analysis fits well the observation that the deletion disrupting a presumed Ca^{2+}-binding motif not only diminishes Ca^{2+} activation but also weakens the observed mechanosensitivity, as expected from the dramatic decrement of the Ca^{2+} activation energy term in the sum (Fig. 3). The mutants with strategic amino acid insertions selectively attenuate the Ca^{2+} activation to a degree that enough synergism can be preserved to manifest the observed near normal mechanosensitivity (Fig. 4). Since we do not yet have the crystal structure of TRP channels, it seems premature to envision how such insertions attenuate Ca^{2+} activation. Experiments are needed to examine other insertions toward understanding how the gating force of Ca^{2+} binding may reach the gate. Strategic insertions reducing gating force are known in the BK linker study (Niu et al. 2004). Regardless of the mechanism, the key observation here is that such insertions further support the parallel model of Ca^{2+} activation and stretch-force activation. We think the energy of Ca^{2+} binding simply converges at the gate together with mechanical energy rather than sensitizing the perception and transmission of the mechanical force to the gate. In order to respond to mild environmental mechanical stimuli, yeast cells may have evolved to enhance the TRPY1 response by Ca^{2+} activation through CICR feedback.

Since TRPY1 can be activated instantly by membrane stretch force in excised patches, energy- or enzyme-dependent pathways are probably not required for its force activation. Furthermore, multiple lines of high-throughput screens, including yeast two-hybrid screens as well as yeast single-gene deletion collection screens, in search for possible interacting partner proteins of TRPY1, did not find any candidate (Loukin et al. 2008). Thus, it seems likely that TRPY1 itself directly senses the stretch force through the membrane, as is the case with MscL, the bacterial mechanosensitive channel (Kung 2005; Martinac et al. 2008). A recent cryo-electron microscope structural study of TRPV1 has shed light on the general organization of TRP channels (Moiseenkova-Bell et al. 2008). In this structure, the transmembrane domains appear to be buried in the lipid bilayer like a balloon and the cytoplasmic domains form a gondola underneath in the cytoplasm. By analogy to the crystal structure of MthK, the balloon and the gondola are tethered through C-terminal peptide linkers (Jiang et al. 2002). Taking together our analysis of gating energetics, our mutational analyses as well as the cryo-electron microscopic image of TRP channels (Moiseenkova-Bell et al. 2008), we propose a mechanistic model for TRPY1 in which the mechanical force acts through the membrane-associated domains (the balloon) and Ca^{2+} binds to the negative charge residues in the cytoplasmic domains (the gondola), both generating energy that reaches the gate in parallel (Fig. 5).

TRPY1 is being developed as a model to understand TRP channels in general. Sorting out the interaction of various gating forces in these polymodal channels is a challenge. Of particular interest is mechanosensitivity, given its importance and the current state of molecular understanding. Clarifying how Ca^{2+} and stretch force gate TRPY1 should facilitate the molecular dissection of this molecule through forward and reverse genetics (Su et al. 2007; Zhou et al. 2007), for which the yeast system is especially suitable.
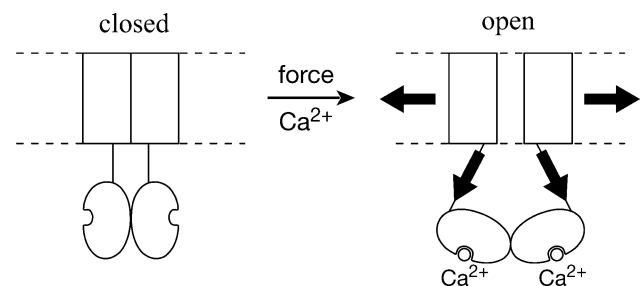

Fig. 5 A mechanistic model of TRPY1 gating by force and by Ca^{2+}. This channel senses membrane stretch force through membrane-buried domains and senses Ca^{2+} via the cytoplasmic gondola. The two gating principles act on the gate in parallel

References

Bandell M, Dubin AE, Petrus MJ, Orth A, Mathur J, Hwang SW, Patapoutian A (2006) High-throughput random mutagenesis screen reveals TRPM8 residues specifically required for activation by menthol. Nat Neurosci 9:493–500

Batiza AF, Schulz T, Masson PH (1996) Yeast respond to hypotonic shock with a calcium pulse. J Biol Chem 271:23357–23362

Bertl A, Slayman CL (1990) Cation-selective channels in the vacuolar membrane of *Saccharomyces*: dependence on calcium, redox state, and voltage. Proc Natl Acad Sci USA 87:7824–7828

Christensen AP, Corey DP (2007) TRP channels in mechanosensation: direct or indirect activation? Nat Rev Neurosci 8:510–521

Cox DH, Cui J, Aldrich RW (1997) Allosteric gating of a large conductance Ca-activated K⁺ channel. J Gen Physiol 110:257–281

Denis V, Cyert MS (2002) Internal Ca²⁺ release in yeast is triggered by hypertonic shock and mediated by a TRP channel homologue. J Cell Biol 156:29–34

Doerner JF, Gisselmann G, Hatt H, Wetzel CH (2007) Transient receptor potential channel A1 is directly gated by calcium ions. J Biol Chem 282:13180–13189

Geiser JR, van Tuinen D, Brockerhoff SE, Neff MM, Davis TN (1991) Can calmodulin function without binding calcium? Cell 65:949–959

Grandl J, Hu H, Bandell M, Bursulaya B, Schmidt M, Petrus M, Patapoutian A (2008) Pore region of TRPV3 ion channel is specifically required for heat activation. Nat Neurosci 11:1007–1013

Ho SN, Hunt HD, Horton RM, Pullen JK, Pease LR (1989) Site-directed mutagenesis by overlap extension using the polymerase chain reaction. Gene 77:51–59

Hofmann T, Chubanov V, Gudermann T, Montell C (2003) TRPM5 is a voltage-modulated and Ca²⁺-activated monovalent selective cation channel. Curr Biol 13:1153–1158

Honore E (2007) The neuronal background K2P channels: focus on TREK1. Nat Rev Neurosci 8:251–261

Horrigan FT, Aldrich RW (2002) Coupling between voltage sensor activation, Ca²⁺ binding and channel opening in large conductance (BK) potassium channels. J Gen Physiol 120:267–305

Hurst AC, Petrov E, Kloda A, Nguyen T, Hool L, Martinac B (2008) MscS, the bacterial mechanosensitive channel of small conductance. Int J Biochem Cell Biol 40:581–585

Jiang Y, Lee A, Chen J, Cadene M, Chait BT, MacKinnon R (2002) Crystal structure and mechanism of a calcium-gated potassium channel. Nature 417:515–522

Kung C (2005) A possible unifying principle for mechanosensation. Nature 436:647–654

Latorre R, Brauchi S (2006) Large conductance Ca²⁺-activated K⁺ (BK) channel: activation by Ca²⁺ and voltage. Biol Res 39:385–401

Launay P, Fleig A, Perraud AL, Scharenberg AM, Penner R, Kinet JP (2002) TRPM4 is a Ca²⁺-activated nonselective cation channel mediating cell membrane depolarization. Cell 109:397–407

Loukin S, Zhou X, Kung C, Saimi Y (2008) A genome-wide survey suggests an osmoprotective role for vacuolar Ca²⁺ release in cell wall-compromised yeast. FASEB J 22:2405–2415

Magleby KL (2003) Gating mechanism of BK (Slo1) channels: so near, yet so far. J Gen Physiol 121:81–96

Martinac B, Saimi Y, Kung C (2008) Ion channels in microbes. Physiol Rev 88:1449–1490

McHugh D, Flemming R, Xu SZ, Perraud AL, Beech DJ (2003) Critical intracellular Ca²⁺ dependence of transient receptor potential melastatin 2 (TRPM2) cation channel activation. J Biol Chem 278:11002–11006

Moiseenkova-Bell VY, Stanciu LA, Serysheva II, Tobe BJ, Wensel TG (2008) Structure of TRPV1 channel revealed by electron cryomicroscopy. Proc Natl Acad Sci USA 105:7451–7455

Nilius B, Vriens J, Prenen J, Droogmans G, Voets T (2004) TRPV4 calcium entry channel: a paradigm for gating diversity. Am J Physiol 286:C195–C205

Nilius B, Prenen J, Tang J, Wang C, Owsianik G, Janssens A, Voets T, Zhu MX (2005) Regulation of the Ca²⁺ sensitivity of the nonselective cation channel TRPM4. J Biol Chem 280:6423–6433

Niu X, Qian X, Magleby KL (2004) Linker-gating ring complex as passive spring and Ca²⁺-dependent machine for a voltage- and Ca²⁺-activated potassium channel. Neuron 42:745–756

Palmer CP, Zhou XL, Lin J, Loukin SH, Kung C, Saimi Y (2001) A TRP homolog in *Saccharomyces cerevisiae* forms an intracellular Ca²⁺-permeable channel in the yeast vacuolar membrane. Proc Natl Acad Sci USA 98:7801–7805

Pedersen SF, Owsianik G, Nilius B (2005) TRP channels: an overview. Cell Calcium 38:233–252

Ramsey IS, Delling M, Clapham DE (2006) An introduction to TRP channels. Annu Rev Physiol 68:619–647

Saimi Y, Kung C (2002) Calmodulin as an ion channel subunit. Annu Rev Physiol 64:289–311

Su Z, Zhou X, Haynes WJ, Loukin SH, Anishkin A, Saimi Y, Kung C (2007) Yeast gain-of-function mutations reveal structure–function relationships conserved among different subfamilies of transient receptor potential channels. Proc Natl Acad Sci USA 104:19607–19612

Venkatachalam K, Montell C (2007) TRP channels. Annu Rev Biochem 76:387–417

Voets T, Droogmans G, Wissenbach U, Janssens A, Flockerzi V, Nilius B (2004) The principle of temperature-dependent gating in cold- and heat-sensitive TRP channels. Nature 430:748–754

Wada Y, Ohsumi Y, Tanifuji M, Kasai M, Anraku Y (1987) Vacuolar ion channel of the yeast, *Saccharomyces cerevisiae*. J Biol Chem 262:17260–17263

Wang YY, Chang RB, Waters HN, McKemy DD, Liman ER (2008) The nociceptor ion channel TRPA1 is potentiated and inactivated by permeating calcium ions. J Biol Chem 283:32691–32703

Zhou X, Su Z, Anishkin A, Haynes WJ, Friske EM, Loukin SH, Kung C, Saimi Y (2007) Yeast screens show aromatic residues at the end of the sixth helix anchor transient receptor potential channel gate. Proc Natl Acad Sci USA 104:15555–15559

Zhou XL, Batiza AF, Loukin SH, Palmer CP, Kung C, Saimi Y (2003) The transient receptor potential channel on the yeast vacuole is mechanosensitive. Proc Natl Acad Sci USA 100:7105–7110

Zurborg S, Yurgionas B, Jira JA, Caspani O, Heppenstall PA (2007) Direct activation of the ion channel TRPA1 by Ca²⁺. Nat Neurosci 10:277–279